Susceptibility Mapping in the Human Brain at 3 and 7T

S. J. Wharton[1], A. Schäfer[2], and R. Bowtell[1]

[1]Sir Peter Mansfield Magnetic Resonance Centre, School of Physics and Astronomy, University of Nottingham, Nottingham, United Kingdom, [2]Department of Neurophysics, Max Planck Institute for Human Cognitive and Brain Sciences, Leipzig, Germany

Introduction: Phase images generated using gradient echo techniques at high field strengths show excellent contrast related to the different magnetic susceptibilities of various brain tissues [1,2]. However, extraction of accurate anatomical information from these images is made difficult by the non-local relationship between the field perturbation and the associated susceptibility distribution [3]. Here, we present a Fourier-based method for calculating 3D susceptibility maps from phase image data. We describe a validation of this approach by analysis of data from a phantom containing different compartments of known susceptibility and the results produced by applying the method to real brain data acquired at 3T and 7T are also discussed.

Methods: In the Fourier domain, the field perturbation, $\Delta B_z(\mathbf{r})$, produced by a susceptibility distribution, $\chi(\mathbf{r})$, that is exposed to a magnetic field, B_0, is given by a simple local expression that is a function of the angle, β, between the **k**-vector and the static magnetic field [3]. Rearranging this expression yields $\chi(\mathbf{k})$ as a function of $\Delta B_z(\mathbf{k})$ (Eq.1). The susceptibility distribution, $\chi(\mathbf{r})$, can therefore be calculated by: (i) measuring $\Delta B_z(\mathbf{r})$ from a phase map, (ii) substituting the Fourier transform of $\Delta B_z(\mathbf{r})$ into Eq.[1] and (iii) applying an inverse Fourier transform to the resulting $\chi(\mathbf{k})$ distribution. There is however a problem with this approach, since the denominator in Eq.[1] tends to zero at the conical surface where $\beta = 54.7^o$. This problem can be avoided by measuring $\Delta B_z(\mathbf{k})$ with the object arranged at different orientations relative to B_0 and then discarding voxels with denominator values less than a given threshold, α, before averaging $\chi(\mathbf{k})$ over orientations. The quality of the final averaged $\chi(\mathbf{k})$ depends upon the range of angles, $\Delta\theta$, through which the object is rotated: larger values turn the conical surface further from its original orientation, so that a larger proportion of k-space is well-defined after averaging. In the case where $\Delta B_z(\mathbf{r})$ is measured at just two angles, the optimum value of $\Delta\theta$ is 45^o which minimises the overlap of the two cones. To test this approach we constructed a spherical, agar phantom containing small, randomly-oriented cylinders of agar doped with two different concentrations (0.5mM and 1mM) of an iron oxide contrast agent. The associated $\Delta\chi$ for this agent was measured separately to be 0.09 ± 0.01 ppm/mM at 7T. For the brain data the red nucleus (RN) and substantia nigra (SN) were targeted at 3T and 7T, as these structures show strong field-shift effects attributed to high iron concentrations [1]. The 7T images were acquired on a Philips Achieva scanner using a 3D spoiled GE FLASH sequence with 0.5 mm isotropic resolution, 128x128x65mm^3/200x200x50mm^3 FOV for the phantom/brain, TE/TR = 16/45 ms for phantom and 20/45 ms for brain, and a flip angle of 16^o. The 3T head images were acquired on a Philips system using a similar protocol with TE/TR = 45/74 ms, and 0.65mm isotropic resolution. The phantom was imaged at angles of -47, -24, and -1^o to B_0 to give $\Delta\theta$ =23 and 46^o. Two healthy subjects were imaged at two orientations to B_o with $\Delta\theta \approx 25\pm7^o$ (rotation about a left-right axis) at both field strengths. The corresponding magnitude images were used to co-register the unwrapped phase images. Regions of interest were masked and high-pass filtered via subtraction of low order 3D polynomials to remove large scale externally generated field perturbations. The phase was then scaled by (γTE) to give field-shift values, before the Fourier transformations and susceptibility calculations were carried out.

$$\chi(\mathbf{k}) = \frac{\Delta B_z(\mathbf{k})}{B_0\left(\frac{1}{3} - \cos^2\beta\right)} \quad \text{Eq.1}$$

Results: Representative slices taken from 3D χ-maps calculated from the phantom data are shown in Fig.1 along with magnitude and phase data acquired at one orientation. The results show that increasing $\Delta\theta$ reduces artefacts (white arrows in C-E) in the final χ-map. The values of $\Delta\chi$ for the 0.5mM and 1mM doped cylinders were calculated from the $\Delta\theta = 46^o$ χ-map as 0.05±0.02ppm and 0.10±0.02ppm respectively, in good agreement with the expected values. In contrast to the χ-maps, the raw phase data shows significant heterogeneity within compartments of uniform susceptibility. The threshold values that gave the best compromise between high contrast and good homogeneity, were found to be $\alpha \approx$ 0.10, 0.11, and 0.13 for $\Delta\theta$=0, 23, and 46^o respectively. Coronal slices taken from the χ-maps created from real brain data at 3 and 7T for one subject are shown in Fig.2(b,d). The RN and SN appear as clear localised structures, in stark contrast to the phase images (Fig.2a,c) that appear to be dominated by non-local fields projected outside of the structures. The calculated $\Delta\chi$ values for the RN and SN relative to the surrounding white matter are summarised in Table.1. The SN has a higher (more paramagnetic) susceptibility than the RN, presumably reflecting a higher concentration of iron. The consistency of the results obtained at 3T and 7T indicates that there is little, if any, saturation of the magnetisation in these structures.

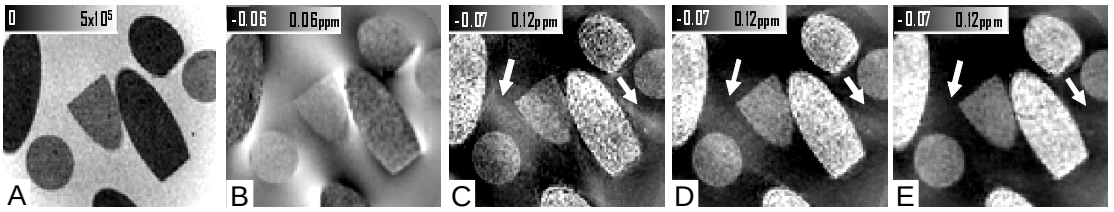

Fig.1 –Phantom data from a representative slice showing magnitude (A) and phase variation (B) at a single orientation along with χ-maps from a single orientation (C) and two-orientations with $\Delta\theta = 23^o$(D) or 46^o(E).

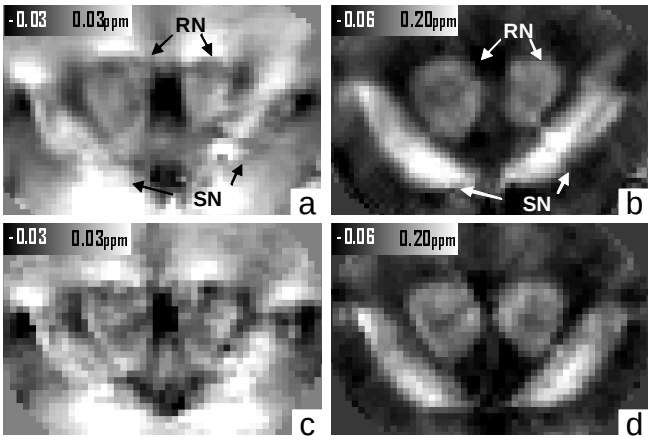

Fig.2 – Phase images (a,c) and susceptibility maps (b,d) at 7T (top) and 3T (bottom).

	Subject.1		Subject.2	
	7T	3T	7T	3T
RN $\Delta\chi$(ppm)	0.08±0.02	0.08±0.03	0.12±0.03	0.14±0.03
SN $\Delta\chi$(ppm)	0.17±0.03	0.16±0.04	0.15±0.03	0.18±0.04

Table.1 – $\Delta\chi$ values relative to surrounding white matter.

Discussion and Conclusions: A robust method for using phase image data to map the susceptibility distribution in samples with complex geometries has been presented. The method was validated using a phantom, then applied successfully to real brain data at 7T and, despite the reduced SNR associated with lower field strengths, sufficient phase information remained at 3T to produce high quality χ-maps. Further work is currently being carried out to optimise the inversion process, so as to allow this promising source of quantitative contrast to be fully exploited.

References: [1] EM Haacke et al. 2005. MRI 23:1-25 [2] JH Duyn et al. 2007. PNAS 104:11796-11801 [3] JP Marques et al. 2005. Conc MR 25B:65-7